Malaysian Journal of Analytical Sciences, Vol 20 No 3 (2016): 633 - 641
DOI: http://dx.doi.org/10.17576/mjas-2016-2003-24

MALAYSIAN JOURNAL OF ANALYTICAL SCIENCES
Published by The Malaysian Analytical Sciences Society
ISSN 1394 - 2506

CONDUCTIVITY AND THERMAL STABILITY OF SOLID ACID COMPOSITES $CsH_2PO_4/NaH_2PO_4/SiO_2$

(Konduktiviti dan Kestabilan Terma Asid Pepejal Komposit $CsH_2PO_4/NaH_2PO_4/SiO_2$)

Norsyahida Mohammad[1], Abu Bakar Mohamad[1, 2], Abdul Amir Hassan Kadhum[2], Loh Kee Shyuan[1]*

[1]*Fuel Cell Institute*
[2]*Department of Chemical and Process Engineering, Faculty of Engineering and Built Environment*
Universiti Kebangsaan Malaysia, 43600 UKM Bangi, Selangor, Malaysia

**Corresponding author: ksloh@ukm.edu.my*

Received: 5 February 2016; Accepted: 22 April 2016

Abstract

Solid acid composites $CsH_2PO_4/NaH_2PO_4/SiO_2$ with different mole ratios of CsH_2PO_4 and NaH_2PO_4 to SiO_2 were synthesized and characterized. Preliminary infrared measurements of CsH_2PO_4 and its composites indicated that hydrogen bonds breaking and formation were detected between 1710 to 2710 cm^{-1}, while the rotation of phosphate tetrahedral anions occurred between 900 and 1200 cm^{-1}. The superprotonic transition of $CsH_2PO_4/NaH_2PO_4/SiO_2$ composite was identified at superprotonic temperatures between 230 and 260 °C, under atmospheric pressure. This study reveals higher conductivity values for composites with higher CsH_2PO_4 (CDP) content. Solid acid composite CDP 613 appeared as the composite with the highest conductivity that is 7.2 x 10^{-3} S cm^{-1} at 230 °C. Thermal stability of the solid acid composites such as temperature of dehydration, melting and decomposition were investigated. The addition of NaH_2PO_4 lowers the dehydration temperature of the solid acid composites.

Keywords: solid acid, conductivity, thermal analysis, caesium dihydrogen phosphate, fuel cell

Abstrak

Asid pepejal komposit $CsH_2PO_4/NaH_2PO_4/SiO_2$ dengan nisbah mol CsH_2PO_4 kepada SiO_2 dan NaH_2PO_4 kepada SiO_2 yang berbeza telah disintesis dan dicirikan dalam ujikaji ini. Pencirian awal sinar inframerah menunjukkan bahawa pemecahan dan pembentukan ikatan hidrogen dikesan antara 1710 cm^{-1} dan 2710 cm^{-1}, manakala putaran anion tetrahedron fosfat berlaku diantara 900 cm^{-1} dan 1200 cm^{-1}. Fasa peralihan berkonduktiviti tinggi bagi asid pepejal komposit $CsH_2PO_4/NaH_2PO_4/SiO_2$ telah dikenal pasti antara suhu 230 hingga 260 °C, di bawah tekanan atmosfera. Nilai kekonduksian proton adalah lebih tinggi bagi komposit yang mempunyai kandungan CsH_2PO_4 (CDP) yang lebih tinggi. Asid pepejal komposit CDP 613 telah muncul sebagai komposit dengan kekonduksian tertinggi iaitu 7.2 x 10^{-3} S cm^{-1} pada suhu 230 °C. Kestabilan terma asid pepejal komposit seperti suhu dehidrasi, takat lebur dan penguraian telah dikenal pasti melalui analisis termogravimetri dan kalorimeter imbasan perbezaan. Penambahan NaH_2PO_4 merendahkan suhu dehidrasi asid pepejal komposit.

Kata kunci: asid pepejal, kekonduksian, analisa terma, sesium dihidrogen fosfat, sel bahanapi

Introduction

Solid acids emerged as a potential solid electrolyte for fuel cell applications due to its high proton conductivity, also known as superprotonic conductivity as the conductivity values increases by 2 to 3 orders of magnitude at intermediate temperatures between 100 to 250 °C, accompanied by phase transition [1]. Solid acids are defined by the basic chemical formula $M_aH_b(XO_4)_c$ where M is a monovalent or divalent metal cation, XO_4 is a tetrahedral oxy-anion, and a, b, c are integers [2]. Solid acids caesium dihydrogen phosphate, CsH_2PO_4 (CDP) and caesium

hydrogen sulphate, $CsHSO_4$ (CHS) have high conductivity values of 2.2 x 10^{-2} S cm^{-1} at 240 °C [3, 4] and 10^{-2} S cm^{-1} at 141 °C [1], respectively. They are comparable to Nafion®, a perfluorosulfonic acid polymer with conductivity value ranging from 9 x 10^{-3} S cm^{-1} to 1.2 x 10^{-1} S cm^{-1} [1, 5] between 80 °C and 100 °C [6], which has been commercialized for application in proton exchange membrane fuel cells (PEMFC), direct methanol fuel cell(DMFC) [7] and micro DMFC [8] due to its stability and robustness.

The disadvantage of Nafion membrane is that humidification is needed during operation of the fuel cell, hence limit the operating temperature to about 100 °C. This escalates the issues of catalyst inefficiency and intolerance to carbon monoxide associated with PEMFC working at low temperatures. Therefore, solid acid emerged as a potential alternative to Nafion as it is able to operate without hydration at higher temperatures, which lowers the operating costs and eliminate the issues of catalyst inefficiency due to carbon monoxide poisoning associated with PEMFC working at low temperatures [9].

It has been found that solid acids with sulphates (SO_4) and selenates (SeO_4) gradually decompose in hydrogen-rich surroundings [10], producing H_2S and H_2Se that are poison to the Pt catalyst at the anode [11, 12] and is further accelerated by the presence of anode catalyst [1]. CHS reacts in hydrogen-rich surroundings to produce H_2S such as in Equation 1.

$$2CsHSO_4 + 4H_2 \rightarrow Cs_2SO_4 + 4H_2O + H_2S \quad (1)$$

Studies have been focusing on CDP [3, 4, 13, 14] due to its stability in hydrogen-rich surroundings. Solid acid is mixed with another solid acid and/or a hygroscopic oxide to produce a solid acid composite with higher conductivity values and improved thermal properties and stability. Two or more solid acids are mixed to widen the temperature range of superprotonic conductivity and induce superprotonic conductivity in solid acids without superprotonic conductivity at atmospheric pressure [15]. Martsinkevich and Ponomareva [16] in the study of CDP partially substituted with sodium dihydrogen phosphate, NaH_2PO_4 (SDP) found that mixed salt solid acid $Cs_{1-x}Na_xH_2PO_4$ with x value up to 0.2 increases the low temperature conductivity of CDP up to 2 orders of magnitude. This study investigates the effect of adding SDP into the CDP/SiO_2 composite. Addition of hygroscopic oxides such as silica (SiO_2), ZrO_2, TiO_2 and Al_2O_3 produces solid acid composites which are more robust and less brittle [2, 15]. The hydrophilic property of SiO_2 enhance proton conductivity of the solid acid composite CDP/SiO_2 [17, 18] and the structure of SiO_2 matrix in the composites of CDP/Al_2O_3 [15] and CDP/SiP_2O_7 [19] enhance the thermal stability of the composites.

Studies on CDP composites include synthesis and characterization of CDP/SiO_2 such as phase transition and proton transport characteristics [20], effects of different types of silica material [18] and different models of protonic conductivity at the ionic salt and oxide interface [21]. In this study, we investigate the properties of solid acid composite $CsH_2PO_4/NaH_2PO_4/SiO_2$, such as the conductivity of the composite via electrochemical impedance spectroscopy, functional groups identification via Fourier-transform infrared spectroscopy and thermal stability via thermogravimetric analysis and differential scanning calorimetry.

Materials and Methods

CDP was synthesized by mixing stoichiometric amounts of caesium carbonate, Cs_2CO_3 (ReagentPlus®, ≥ 99% Sigma Aldrich) and phosphoric acid H_3PO_4 (≥85 wt% in H_2O, Sigma Aldrich) according to the following reaction (Equation 2):

$$Cs_2CO_3 + 2H_3PO_4 \rightarrow 2CsH_2PO_4 + CO_2 + H_2O \quad (2)$$

In CDP synthesis, measured amount of Cs_2CO_3 was dissolved in distilled water. Surfactant powder, Cetyltrimethylammoniumbromide, CTAB (BioXtra®, ≥ 99 % Sigma Aldrich) was dissolved in ethanol separately and added to the Cs_2CO_3 solution to reduce water surface tension and hence assist particle dispersion. The mixture was then stirred for 10 minutes until clear solution was produced. Phosphoric acid was added, drop-wise into the mixture with continuous stirring for another 10 minutes. Acetone is added excessively to the mixture while stirring for another 30 minutes and the solution is vacuum-filtered to produce CDP in the form of white precipitate. The

white precipitate is washed several times by mixing with excess acetone and vacuum-filtered to remove remaining surfactants. The synthesized CDP is dried at 130 °C for 24 hours to eliminate absorbed water and grinded to produce powdered CDP.

Solid acid composites $CsH_2PO_4/NaH_2PO_4/SiO_2$ of different molar ratios as tabulated in Table 1 were synthesized via the sol gel method, the similar method used synthesize electrolyte of a solid oxide fuel cell[22]. The synthesized CDP and NaH_2PO_4, SDP (ReagentPlus®, ≥ 99 % Sigma Aldrich) powders were mixed prior addition to tetraethyl orthosilicate, TEOS solution. TEOS solution was prepared by mixing TEOS (Reagent Grade®, 98 % Sigma Aldrich) with ethanol, water and hydrochloric acid (1 mol L^{-1}, Merck) in mole ratio of 1:8:30:0.05. The solid acid and TEOS mixture was stirred until all powders were dissolved. The mixture was kept at 40 °C for 24 hours and further dried at 150 °C for 15 hours to produce white precipitate solid acid composite, $CsH_2PO_4/NaH_2PO_4/SiO_2$. The resultant precipitate was then grinded to produce fine solid acid composite powders.

Table 1. Solid acid composites synthesized

Solid acid sample	**CsH_2PO_4:NaH_2PO_4:SiO_2 molar ratio**
CDP 631	6:3:1
CDP 721	7:2:1
CDP 811	8:1:1
CDP 613	6:1:3
CDP 523	5:2:3
CDP 433	4:3:3

Solid acid CDP and its composites were characterized via electrochemical impedance spectroscopy, Fourier-transform infrared spectroscopy, thermogravimetric analysis and differential scanning calorimetry. The solid acids were tested for its protonic conductivity via electrochemical impedance spectroscopy (EIS). The pure CDP and its composite powders were pressed into pellets of 1 mm thickness and 13 mm diameter by uniaxially pressing at 3 tonnes cm^{-2} at room temperature for 1 minute. The pellets were calcined at 260 °C for 1 hour in air, painted with silver (Ag) suspension and heat-treated to improve contacts of the surfaces to the current collector, prior to assembly in the pellet holder for impedance measurements. The pellet was sandwiched between two square platinum meshes which acts as the current collector, placed inside a metal pellet holder with ceramic lining and connected to an Autolab impedance analyser. The impedance readings were taken in air at 180 °C, 210 °C, 230 °C 250 °C and 260 °C with frequency of 1.0 x 10^{-2} to 1.0 x 10^{6} Hz and current of 0.01A. The measured data was analyzed using the Nova software package where the proton conductivity value was determined from the impedance data plotted on real and imaginary axes, Z' and -Z'' respectively, known as Nyquist plot. The curve was fitted using the equivalent circuit as in Figure 1. The proton conductivity value, σ for pure CDP and $CsH_2PO_4/NaH_2PO_4/SiO_2$ composites were calculated using the resistance value, R and is given by the following Equation 3:

$$\text{Conductivity, } \sigma \text{ (S cm}^{-1}) = {}^{1/R(\Omega)}\Big/_{A(cm^2)/l(cm)} \quad (3)$$

Fourier-transform infrared spectroscopy (FTIR) is used to identify functional groups that are present in the solid acid materials. Solid acid samples were mixed with grounded KBr with solid acid to KBr weight ratio of 1 to 300 and pressed into a pellet for FTIR measurements. The spectrum was collected via Perkin-Elmer 125 spectrometer between 200 and 4000 cm^{-1} wavenumbers at room temperature.

Thermal stability of the solid acid materials were measured via thermogravimetric analysis (TGA) and differential scanning calorimetry (DSC). Solid acid decomposition is identified by measuring mass loss as a function of temperature via TGA analysis. DSC measurements display endothermic or exothermic peaks that appear during

heating of the solid acid, which are usually related to the phase transition of solid acid. Both TGA and DSC tests were run simultaneously using STA 449 F3 Netzsch simultaneous TGA-DSC between 30 °C and 600 °C with heating rate of 5 °C min^{-1} under nitrogen flow.

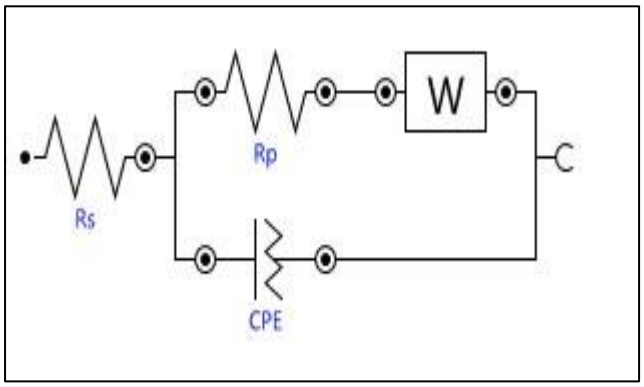

Figure 1. The equivalent circuit used to analyze the impedance data

Results and Discussion

Proton conductivity of $CsH_2PO_4/NaH_2PO_4/SiO_2$ composites

The Nyquist plot for each CDP composite has a similar pattern to the plot for CDP 613 at various temperatures as shown in Figure 2. The semi-circle of the fitted plot represents the impedance of the bulk of the solid acid electrolyte and the straight line represents the semi-infinite diffusion behaviour of the solid-gas interface of the solid acid electrolyte. The conductivity of CDP 613 increases as temperature increases from 180 °C to 210 °C and 230 °C where the conductivity is the highest. However, as temperature is increased to 250 °C and 260 °C, the conductivity drops slightly, indicating that the optimum temperature with highest conductivity value is at 230 °C for CDP 613.

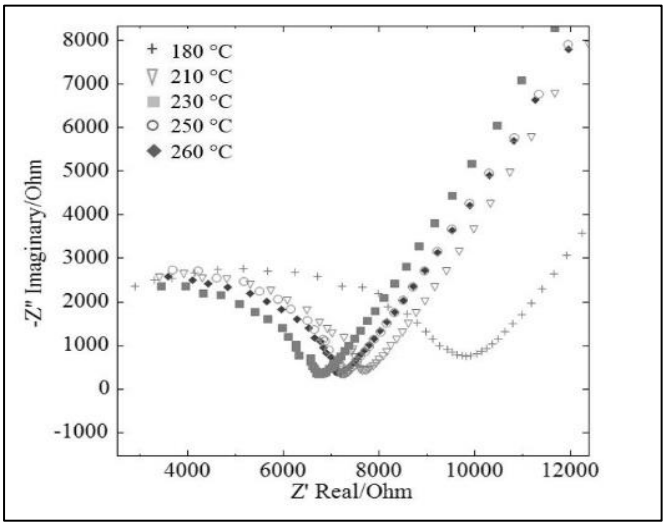

Figure 2. The impedance measurement of CDP 613 at 180 °C, 210 °C, 230 °C, 250 °C and 260 °C plotted in Nyquist plot.

Conductivity measurements were conducted for all CDP composites at 180°C, 210°C, 230°C, 250°C and 260°C. The highest conductivity values of pure CDP and its composites are tabulated in Table 2. It was found that the superprotonic conductivity of pure CDP occurs at about 230 °C with conductivity value of 1.9 x 10^{-2} S cm^{-1}, comparable to proton conductivity value of 2.2 x 10^{-2} S cm^{-1} at 240 °C obtained by Haile et al. [3]. Solid acid composite CDP 613 has the highest conductivity value of 7.2 x 10^{-3} S cm^{-1} at about 230 °C compared to other composites. The conductivity of CDP 613 composite is lower than the conductivity of pure CDP at the same temperature. The presence of SiO_2 which is non-conductive, slightly reduces the conductivity of solid acid composites, due to the imperfect interconnections between the solid acid and SiO_2 [15].

Table 2. The highest conductivity value for each solid acid

Solid acid	**Highest conductivity value, σ (S cm^{-1})**	**T_{sp} (°C)**
CDP [3]	2.2 x 10^{-2}	240
CDP (pure)	1.9 x 10^{-2}	230
CDP 631	5.0 x 10^{-3}	230
CDP 721	1.7 x 10^{-3}	250
CDP 811	8.5 x 10^{-4}	250
CDP 613	7.2 x 10^{-3}	230
CDP 523	2.0 x10^{-3}	260
CDP 433	2.6 x 10^{-3}	250

In previous work by Boysen [2], it was found that SDP alone melts without reaching the superprotonic phase. A recent study by Marsinkevich [16] highlights the effect of adding SDP up to 20 % of CDP/SDP composite, where conductivity increases by 2 orders of magnitude around 160 °C to 200 °C compared to pure CDP. In this study, we found that the addition of SDP into the CDP/SiO_2 composites increases the conductivity value of composites with 10 % SiO_2 that are CDP 631, CDP 721 and CDP 811, whilst reducing the temperature where superprotonic conductivity of the composites occur. The conductivity of $Cs_{1-x}Na_xH_2PO_4$ composite increases by 2 orders of magnitude with x values up to 0.2 at 160 °C to 200 °C, lower than the superprotonic temperature of pure CDP that is 240 °C [16]. This is associated with the structural order-disorder movements caused by Cs^+ and Na^+ cations coexisting within the lattice of the solid acid composites.

Structure and thermal stability of $CsH_2PO_4/NaH_2PO_4/SiO_2$ composites

The infrared spectra of CDP is shown in Figure 3 where well separated peaks were observed at 2710 cm^{-1}, 2310 cm^{-1} and 1710 cm^{-1} which are assigned to the stretching of oxygen-hydrogen bonds in and out of planes also known as the 'ABC bonds of OH', while the strong absorption bands between 900 cm^{-1} and 1200 cm^{-1} were attributed to the internal vibrations of $H_2PO_4^-$ oxyanion that are the vibrations of two main groups PO_2 and $P(OH)_2$. The PO_2 stretching modes result in more intense bands compared to the $P(OH)_2$ stretching modes. The wavelength of PO_2 stretching modes are due to PO_2 symmetric and asymmetric stretching measured at 941 cm^{-1} and 1070 cm^{-1} respectively. Weaker bands of $\delta_{P\text{-}O\text{-}H}$ in-plane bending and $\gamma_{P\text{-}O\text{-}H}$ out-of-plane bending are identified at 1130 cm^{-1} and 1213 cm^{-1} respectively and is comparable to the bands of CDP nanoparticles that are 1140 cm^{-1} and 1185 cm^{-1} respectively [23]. The generated Cs···O-H bond is represented by the peaks within 300 cm^{-1} to 500 cm^{-1} region. The IR spectra of CDP and its composites measured in this work is compared to previous works as in Table 3.

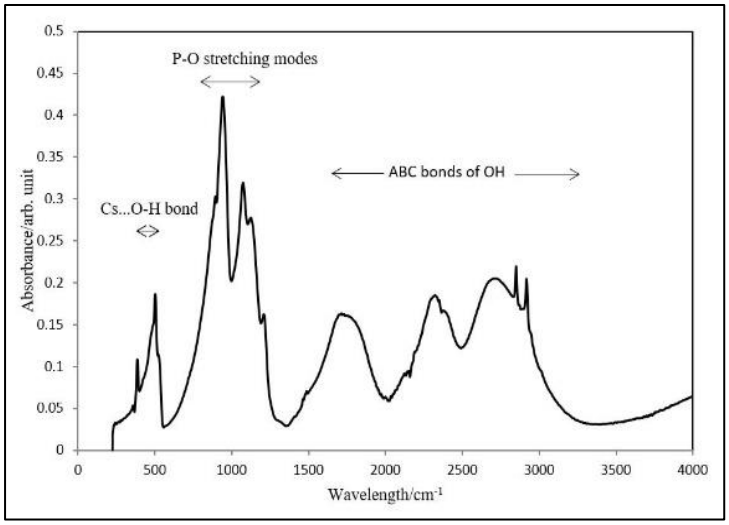

Figure 3. The FTIR absorbance bands for CDP.

Table 3. The comparison of functional groups present in solid acid materials

Solid acid sample	Reference	Wavelength (cm^{-1})					
		Cs …O-H bond	P-O_2 stretching		O-H stretching		
			symmetric	asymmetric			
CDP (pure)	This study	502	941	1070	1710	2310	2710
CDP nanoparticles	[23]	490	940	1070	1650	2300	2650
CDP	[18]	N/A	950	1100	1700	2300	2700

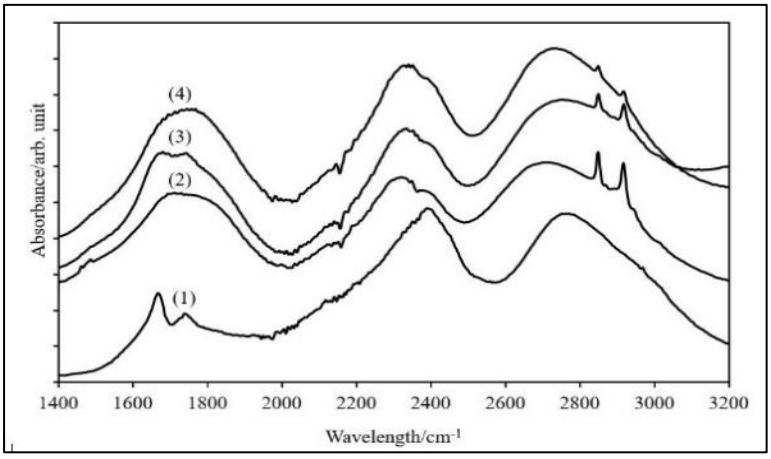

Figure 4. Infrared spectra of (1) sodium dihydrogen phosphate, (2) caesium dihydrogen phosphate, (3) CDP 811 composite and (4) CDP 631 composite.

The FTIR measurement conducted for CDP composites found that the addition of SDP into the solid acid composite did not produce any obvious change in the pattern of the absorbance bands for ABC bonds of OH, as depicted in Figure 4 for CDP 631 and CDP 811. However, it increases the frequency of the absorbance bands slightly, indicating lengthening of P-O¨H and shortening of P-O bonds. This is similar to the trend observed by Martsinkevich and Ponomareva [16].

The DSC measurements for CDP and its composites are presented in Figure 5. Decomposition occurs in these solid acids according to the following dehydration pathway (Equation 4) [24-26]:

$$CsH_2PO_4 \rightarrow Cs_2H_2P_2O_7 \rightarrow CsPO_3 \quad (4)$$

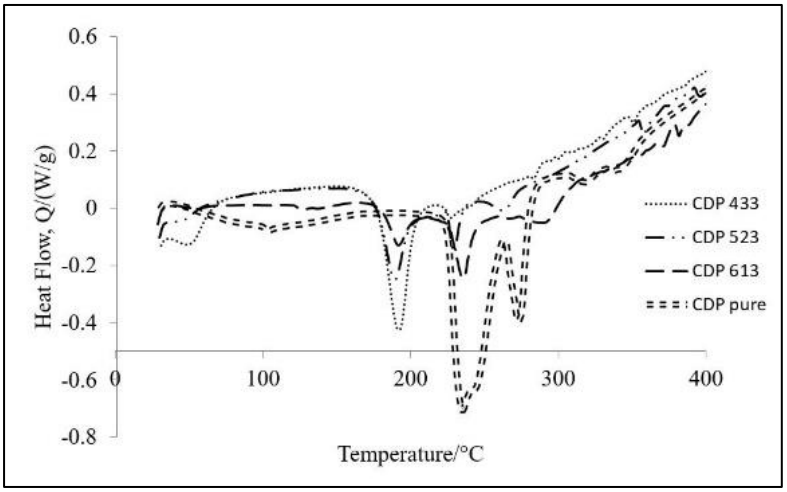

Figure 5. DSC curves for CDP and its composites.

The first reaction pathway ($CsH_2PO_4 \rightarrow Cs_2H_2P_2O_7$) occurs over temperature range of 220 °C to 260 °C due to thermal decomposition of CDP to form another compound, dicaesium dihydrogen pyrophosphate $Cs_2H_2P_2O_7$. This is followed by the formation of $CsPO_3$ around temperature range of 265 °C to 285 °C. At about 320 °C, decomposition occurs. This is in agreement with the findings by Hosseini et al. [24]. The CDP composites that are CDP 433, CDP 523 and CDP 613 with different ratios of SDP and SiO_2 shows two distinctive peaks in DSC measurements at lower temperatures around 190 °C and 230 °C as compared to the DSC curve of pure CDP. The first reaction pathway of the composite producing $Cs_2H_2P_2O_7$ occurs over temperature range of 175 °C to 210 °C followed by the formation of $CsPO_3$ around temperature range of 220 °C to 255 °C, both occurrence at lower temperature than pure CDP.

The lower temperature dehydration of CDP composites may be associated with the presence SDP in the composite. DSC analysis of SDP revealed three distinctive peaks at 60 °C, 210 °C and 345 °C as in Figure 6. It is noteworthy that due to the hygroscopic nature of the solid acid, the first peak at 60 °C represent the release of water molecules at the surface of the solid acids during the DSC measurement. This is supported by thermal analysis of SDP [16], where dehydration peaks were identified at 208 °C and 280 °C. Similarly, prior studies indicated that SDP undergo dehydration at a lower temperature such as at 169 °C [27] and 200 °C [2]. Therefore, by adding SDP into the solid acid composites, dehydration occurs at a lower temperature than pure CDP.

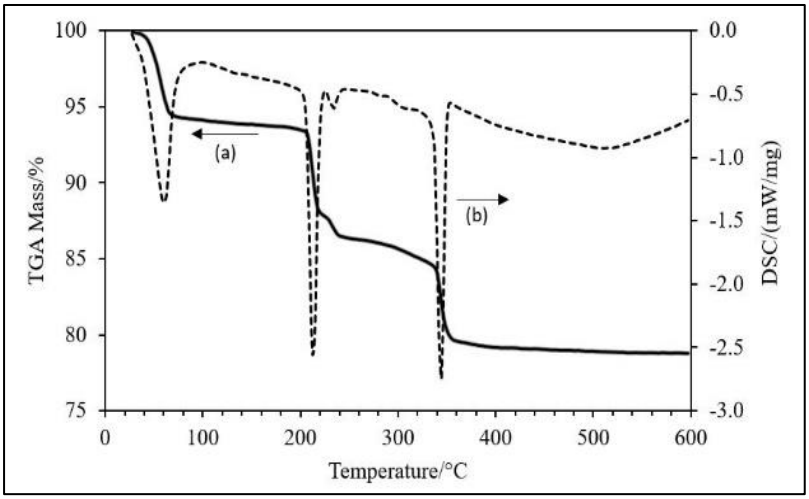

Figure 6. TGA (a) and DSC (b) curves for solid acid NaH_2PO_4, SDP

Conclusion

Conductivity measurements revealed solid acid composite CDP 613 as the composite with the highest conductivity that is 7.2 x 10^{-3} S cm^{-1} at about 230 °C compared to the other composites. This conductivity value is lower than the conductivity of pure CDP due to the defective interconnections between the solid acid and the non-conductive SiO_2 particles. The addition of SDP into the CDP/SiO_2 composites increases the conductivity of composites whilst reducing the temperature at which the superprotonic transition occur. Thermal analysis showed earlier onset of dehydration for CDP/SDP/SiO_2 composites compared to pure CDP, which is most likely due to the presence of SDP which has lower dehydration and melting point. The mechanism of proton transport within CDP was confirmed to occur by breaking and formation of hydrogen bonds and rotation of the phosphate tetrahedron anions, as identified via the FTIR analysis where distinctive peaks were observed from 1710 to 2710 cm^{-1} and 900 to 1200 cm^{-1} respectively.

Acknowledgement

The authors gratefully acknowledge the financial support by the Malaysian Ministry of Higher Education (MOHE) through the Exploratory Research Grant Scheme (ERGS/1/2012/TK07/UKM/01/1) and the Universiti Kebangsaan Malaysia (UKM) through University Research Grant (DLP-2013-038).

References

1. Dupuis, A.-C. (2011). Proton exchange membranes for fuel cells operated at medium temperatures: Materials and experimental techniques. *Progress in Materials Science*, 56(3): 289 - 327.
2. Boysen, D. A. (2004). Superprotonic solid acids: structure, properties, and applications (PhD Dissertation), California Institute of Technology. Retrieved from http://resolver.caltech.edu/CaltechETD:etd-05282004-155105
3. Haile, S. M., Chisholm, C. R. I., Sasaki, K., Boysen, D. A. and Uda, T. (2006). Solid acid proton conductors: from laboratory curiosities to fuel cell electrolytes. *Faraday Discussions*, 134: 17 - 39.
4. Taninouchi, Y.-K., Uda, T., Awakura, Y., Ikeda, A. and Haile, S. M. (2007). Dehydration behavior of the superprotonic conductor CsH_2PO_4 at moderate temperatures: 230 to 260 °C. *Journal of Materials Chemistry*, 17(30): 3182 - 3189.
5. Alberti, G., Casciola, M., Pica, M., Tarpanelli, T. and Sganappa, M. (2005). New preparation methods for composite membranes for medium temperature fuel cells based on precursor solutions of insoluble inorganic compounds. *Fuel Cells*, 5(3): 366 - 374.
6. Peighambardoust, S. J., Rowshanzamir, S. and Amjadi, M. (2010). Review of the proton exchange membranes for fuel cell applications. *International Journal of Hydrogen Energy*, 35(17): 9349 - 9384.

7. Jaafar, J., Ismail, A. F., Matsuura, T. and Norddin, M. N. A. M. (2013). Stability of SPEEK-triaminopyrimide polymer electrolyte membrane for direct methanol fuel cell application. *Sains Malaysiana*, 42(11): 1671 - 1677.
8. Hashim, N., Kamarudin, S. K. and Daud, W. R. W. (2010). Design and development of micro direct methanol fuel cell (μDMFC) for portable application. *Sains Malaysiana*, 39(6): 1015 - 1023.
9. Haile, S. M., Boysen, D. A., Chisholm, C. R. I. and Merle, R. B. (2001). Solid acids as fuel cell electrolytes. *Nature*, 410: 910 - 913.
10. Unnikrishnan, S. (2009). Micromachined dense palladium electrodes for thin-film solid acid fuel cells. (PhD Dissertation), University of Twente, Enschede. Retrieved from http://doc.utwente.nl/68765/
11. Haile, S. M. (2003). Materials for fuel cells, in Materials Today. Elsevier Science Ltd.
12. Merle, R. B., Chisholm, C. R. I., Boysen, D. A. and Haile, S. M. (2002). Instability of sulfate and selenate solid acids in fuel cell environments. *Energy & Fuels*, 17(1): 210 - 215.
13. Botez, C. E., Hermosillo, J. D., Zhang, J., Qian, J., Zhao, Y., Majzlan, J., Chianelli, R. R. and Pantea, C. (2007). High-temperature phase transitions in CsH_2PO_4 under ambient and high-pressure conditions: A synchrotron x-ray diffraction study. *The Journal of Chemical Physics*, 127(19): 194701 -194706.
14. Baranov, A. I., Khiznichenko, V. P. and Shuvalov, L. A. (1989). High temperature phase transitions and proton conductivity in some kdp-family crystals. *Ferroelectrics*, 100(1): 135 - 141.
15. Baranov, A. I., Grebenev, V. V., Khodan, A. N., Dolbinina, V. V. and Efremova, E. P. (2005). Optimization of superprotonic acid salts for fuel cell applications. *Solid State Ionics*, 176(39–40): 2871 - 2874.
16. Martsinkevich, V. V. and Ponomareva, V. G. (2012). Double salts $Cs_{1-x}M_xH_2PO_4$ (M = Na, K, Rb) as proton conductors. *Solid State Ionics*, 225(0): 236 - 240.
17. Otomo, J., Minagawa, N., Wen, C.-j., Eguchi, K. and Takahashi, H. (2003). Protonic conduction of CsH_2PO_4 and its composite with silica in dry and humid atmospheres. *Solid State Ionics*, 156(3–4): 357 - 369.
18. Ponomareva, V. G. and Shutova, E. S. (2007). High-temperature behavior of CsH_2PO_4 and CsH_2PO_4–SiO_2 composites. *Solid State Ionics*, 178(7–10): 729 - 734.
19. Matsui, T., Kukino, T., Kikuchi, R. and Eguchi, K. (2005). An intermediate temperature proton-conducting electrolyte based on a CsH_2PO_4/SiP_2O_7 composite. *Electrochemical and Solid-State Letters*, 8(5): 256 - 258.
20. Otomo, J., Ishigooka, T., Kitano, T., Takahashi, H. and Nagamoto, H. (2008). Phase transition and proton transport characteristics in CsH_2PO_4/SiO_2 composites. *Electrochimica Acta*, 53(28): 8186 - 8195.
21. Naidoo, S. (2004). Cesium Hydrogen Sulphate and Cesium Dihydrogen Phosphate Based Solid Composite Electrolyte for Fuel Cell Application. University of the Western Cape.
22. Panuh, D., Muchtar, A., Muhamad, N., Majlan, E.H. and Daud, W. R. W. (2014). $Sm_{0.2}Ce_{0.8}O_{1.90}$ (SDC)/ $Y_{0.25}Bi_{0.75}O_{1.5}$ (YSB) bilayered electrolytes for intermediate solid oxide fuel cells. *Sains Malaysiana*, 43(11): 1769 - 1774.
23. Hosseini, S., Wan Daud, W.R., Badiei, M., Kadhum, A. A. H. and Mohammad, A. B. (2011). Effect of surfactants in synthesis of CsH_2PO_4 as protonic conductive membrane. *Bulletin of Materials Science*, 34(4): 759 - 765.
24. Hosseini, S., Mohamad, A., Kadhum, A. and Wan Daud, W. R. (2010). Thermal analysis of CsH_2PO_4 nanoparticles using surfactants CTAB and F-68. *Journal of Thermal Analysis and Calorimetry*, (1): 197 - 202.
25. Boysen, D. A., Haile, S. M., Liu, H. and Secco, R. A. (2003). High-Temperature Behavior of CsH_2PO_4 under both ambient and high pressure conditions. *Chemistry of Materials*, 15(3): 727 - 736.
26. Hosseini, S. (2009). Synthesis of proton conducting membrane using cesium dihydrogen phosphate nanoparticles for the fabrication of membrane electrode assembly for fuel cell. Universiti Kebangsaan Malaysia.
27. Gupta, L. C., Rao, U. R. K., Venkateswarlu, K. S. and Wani, B. R. (1980). Thermal stability of CsH_2PO_4. *Thermochimica Acta*, 42(1): 85 - 90.